Cell Stem Cell, Volume *15*
Supplemental Information

Human ESC-Derived Dopamine Neurons Show Similar Preclinical Efficacy and Potency to Fetal Neurons when Grafted in a Rat Model of Parkinson's Disease

Shane Grealish, Elsa Diguet, Agnete Kirkeby, Bengt Mattsson, Andreas Heuer, Yann Bramoulle, Nadja Van Camp, Anselme L. Perrier, Philippe Hantraye, Anders Björklund, and Malin Parmar

SUPPLEMENTAL INFORMATION

Supplemental information includes 6 figures, detailed Supplemental Experimental Procedures and Supplemental References.

Figure S1

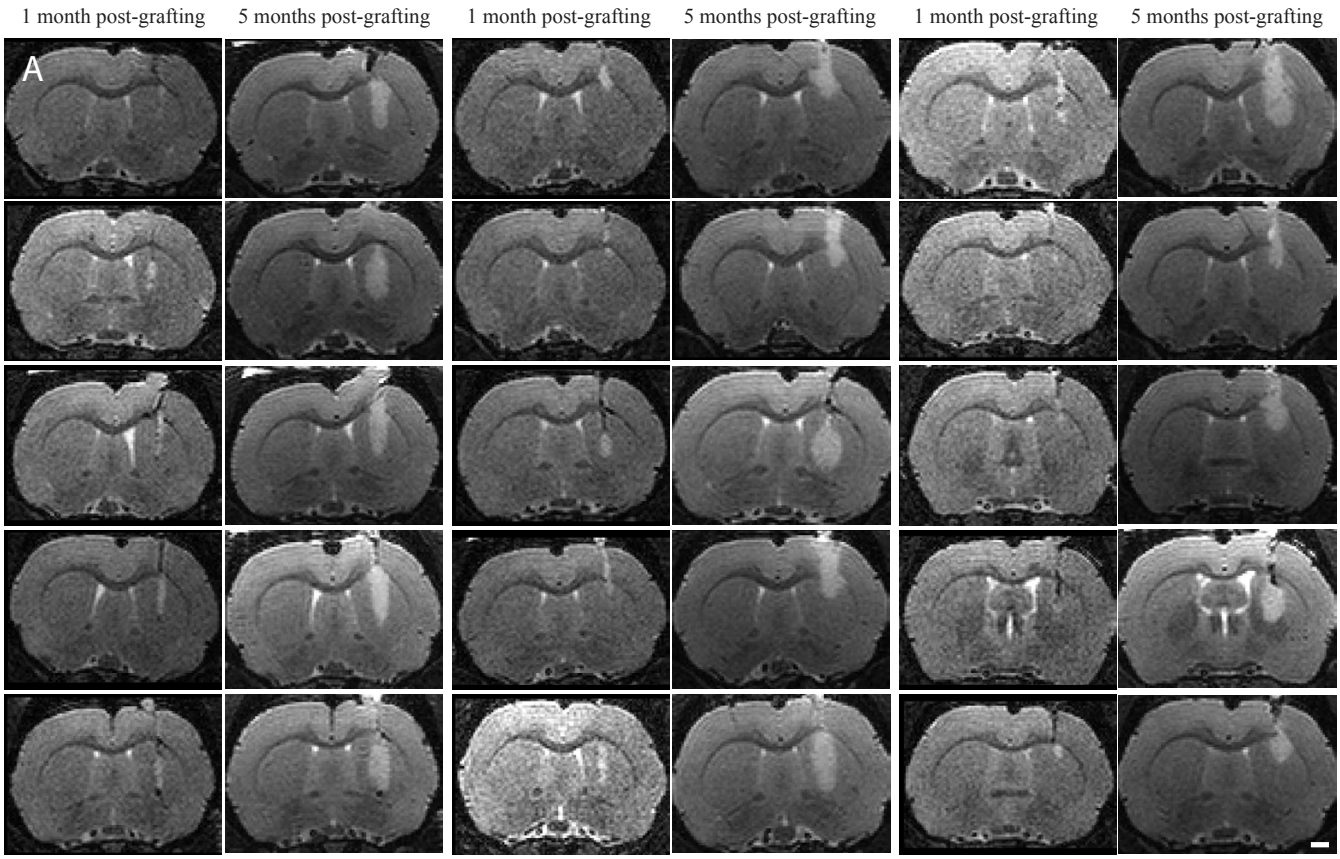

B

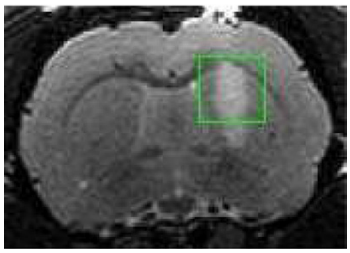

Voxel: 3x3x3mm^3

C

MRS 5M post-transplantation

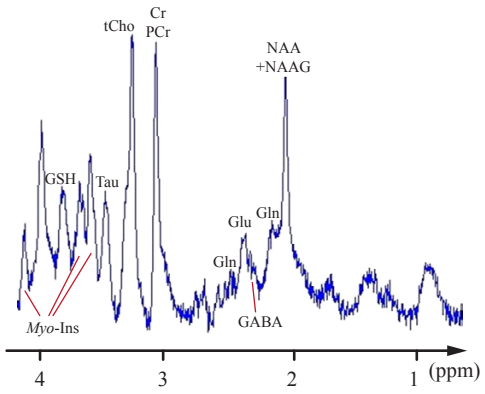

Figure S1 – Related to Figure 1

MRI scans and MR spectroscopy profile of long-term intrastriatal transplants of hESC-DA neurons.

(**A**) MRI scans for each individual animal (n=15) 1 and 5 months post-transplantation reveals well-placed transplants within the striatum that matured and occupied a larger volume over time, in the absence of any gross morphological damage or overgrowth formation. (**B**) Coronal view of the rat brain at the level of the graft, visualized by T2-weighted MRI. The green box delineates the area in which spectra were acquired. (**C**) A typical ^{1}H NMR spectra acquired *in vivo* in the area of the graft. In addition to commonly detected *N*-acetylaspartic acid (NAA, neuronal marker), creatine/phospho-creatine (Cr/PCr) and choline-containing compounds (tCho, membrane turnover marker), short echo-time detection allowed to visualize the presence of glutamate (Glu), Inositol (Myo-Ins, glial marker), taurine (Tau), glutamine (Gln), GABA, GSH (glutathione) within and around the graft, indicative of a normal profile of neurochemical metabolites.

Figure S2

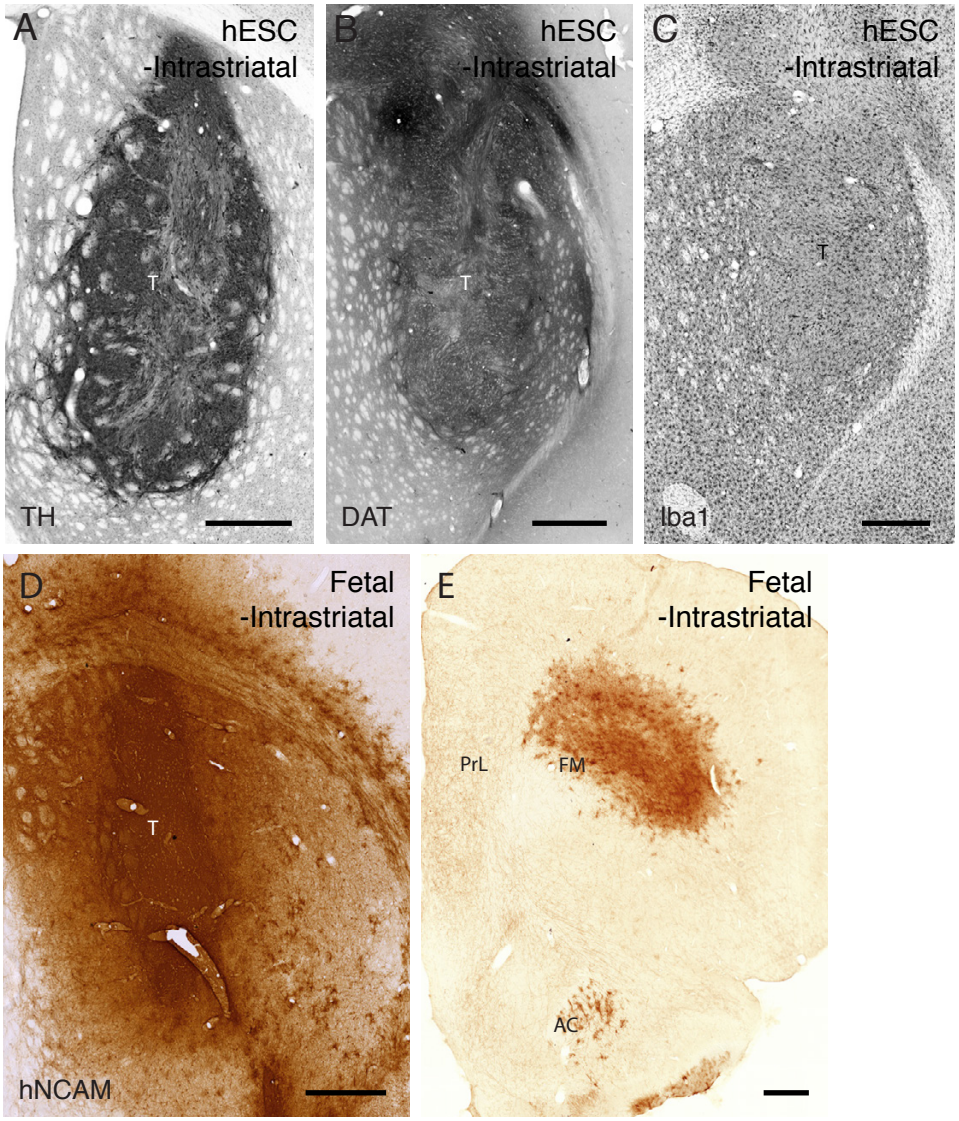
A
hESC
-Intrastriatal
T
TH
B
hESC
-Intrastriatal
T
DAT
C
hESC
-Intrastriatal
T
Iba1
D
Fetal
-Intrastriatal
T
hNCAM
E
Fetal
-Intrastriatal
PrL
FM
AC

Figure S2 – Related to Figure 2

Immunohistochemical analysis of intrastriatal transplants after 6 months survival.

Long-term intrastriatal transplants of hESC-DA neurons that underwent PET imaging contained a large numbers of surviving TH^+ neurons (**A**), and high dopamine transporter DAT levels (**B**), in the absence of any detectable immune response within or surrounding the graft core, as assessed by immunostaining for $Iba1^+$, a marker for activated microglia (**C**). (**D**) Immunostaining for hNCAM of fetal VM grafted to the striatum revealed a large, neuron-rich graft core that provided extensive innervation of the surrounding striatum, as well as being encompassed by a substantial number of $hNCAM^+$ glial cells. (**E**) Graft-derived $hNCAM^+$ fibers could be traced also outside the striatum, innervating areas of the prefrontal cortex, including the prelimbic cortex. A notable observation is the high number of glia migrating along the forceps minor, as shown in (**E**).

AC= anterior commissure; cc= corpus callosum; FM=forceps minor; PrL= prelimbic cortex; T=transplant.

Scale bars: **A-E** = 0.5 mm.

Figure S3


A
Fetal 8 w p.c.
T
hNCAM
B
Fetal 5.5 w p.c.
T
hNCAM
C
Fetal 5.5 w p.c.
IC
MFB
hNCAM
D
Fetal 5.5 w p.c.
MeA
BLA
E
Fetal 5.5 w p.c.
CC
CPu
F
Fetal 5.5 w p.c.
AC
NAc
G
Fetal 5.5 w p.c.
FM
PrL

Figure S3 – Related to Figure 4

Overview of intranigral transplants of fetal VM, 6 months post-transplantation.

(**A, B**) Coronal sections immunostained for hNCAM and visualized under dark-field illumination from intranigral transplants of fetal VM obtained from an 8-week (**A**) and a 5.5-week (**B**) donor. The images in (**A**) were used to generate the schematic in **Figure 4A**. (**C**) Inspection of the MFB revealed that $hNCAM^{+}$ fibers readily course through both gray and white matter. (**D**) Axons exit the MFB laterally to innervate nuclei of the amygdala. (**E**) $hNCAM^{+}$ axons from fetal VM sourced from the 5.5-week donor exhibited a strong preference for the dorsolateral caudate-putamen, as observed with grafts of 8-week VM. (**F**) Specific innervation of A10 target structures, such as NAc. (**G**) Long-distance axonal outgrowth was observed providing innervation of A10 cortical target structures, like prelimbic cortex.

AC= anterior commissure; BLA= basolateral amygdala; CPu= caudate-putamen unit; FM= forceps minor; IC= internal capsule; MeA= medial amygdaloid nucleus; MFB= medial forebrain bundle; NAc= nucleus accumbens; PrL= prelimbic cortex, T= transplant.

Scale bars: **A** and **B** = 1 mm; **C** = 100 μm, **D-G** = 0.5 mm.

Figure S4

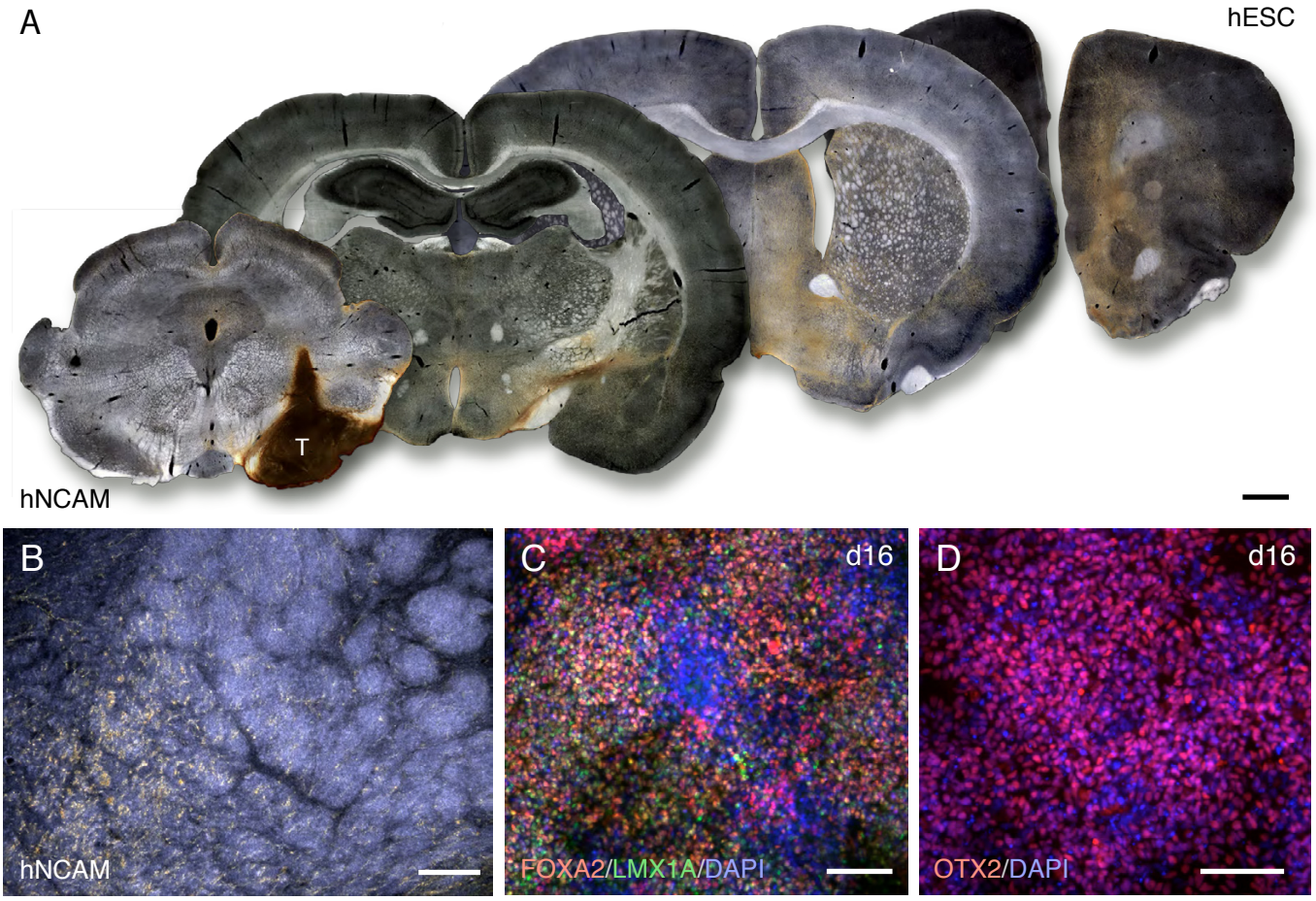

Figure S4 – Related to Figure 5

Overview of intranigral grafted hESC-DA neurons, 6 months survival.

(**A**) Dark-field images of the coronal sections used to generate the schematic in **Figure 5A** showing graft-derived outgrowth visualized using hNCAM immunohistochemistry. (**B**) Close examination of the MFB revealed that $hNCAM^{+}$ fibers coursed through both gray matter and white matter tracts, such as internal capsule. (**C, D**) *In vitro*, the cells used for transplantation, obtained from day 16 of hESC-differentiation, revealed a high co-expression of the midbrain DA progenitor markers FOXA2 and LMX1A (**C**), as well as a high proportion of OTX2 expressing progenitors (**D**).

Scale bars: **A** = 1 mm; **B-D** = 100 μm.

Figure S5

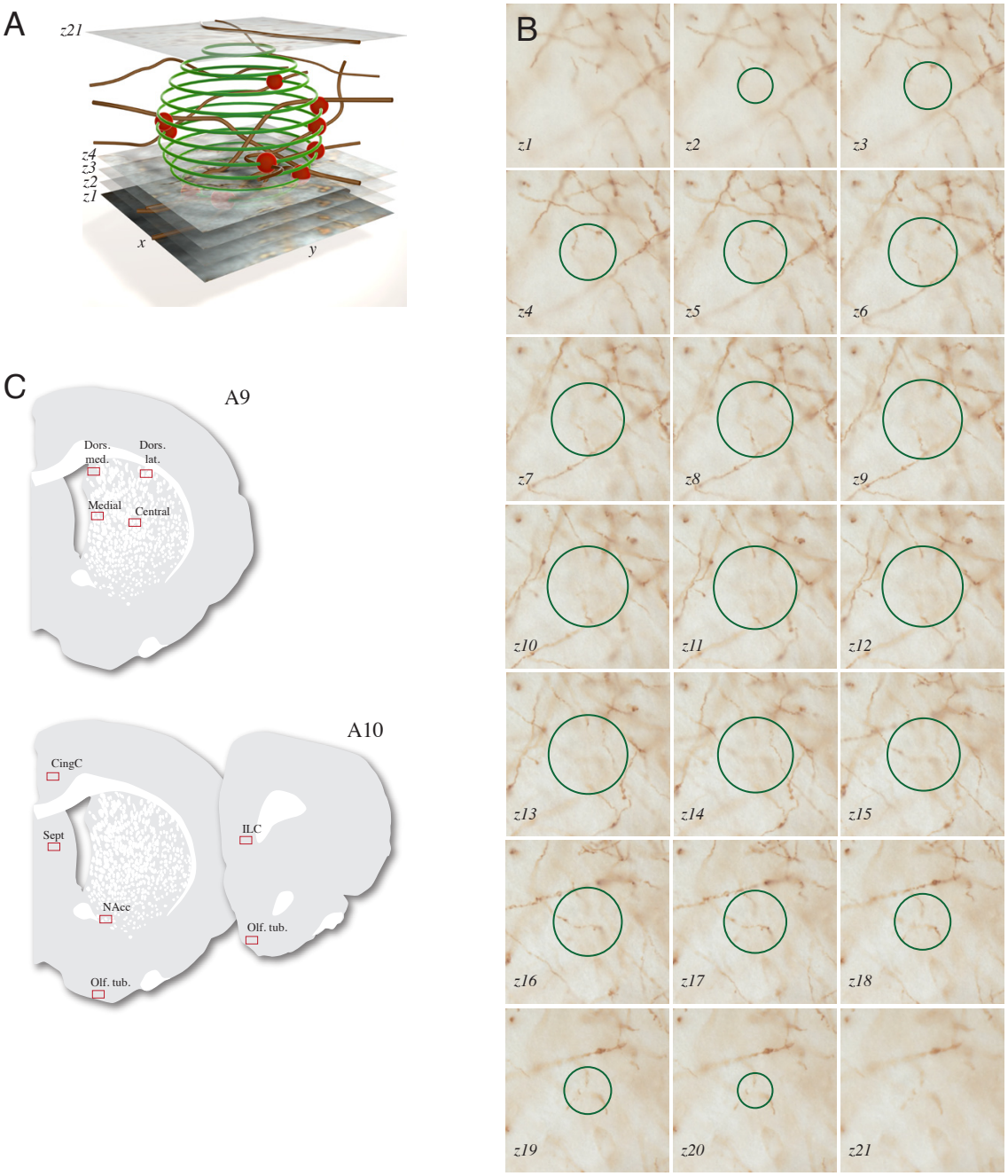
A
z21
z4
z3
z2
z1
x
y
B
z1
z2
z3
z4
z5
z6
z7
z8
z9
z10
z11
z12
z13
z14
z15
z16
z17
z18
z19
z20
z21
C
A9
Dors. med.
Dors. lat.
Medial
Central
A10
CingC
Sept
NAcc
Olf. tub.
ILC
Olf. tub.

Figure S5 – Related to Figure 6

Method used for fiber density measurements in A9 and A10 target structures.

(**A**) "Sphere method" for estimation of the number of fibers passing through a given volume. A z-stack through the whole section is taken at 1µm intervals, after which a sphere with a diameter of 19 µm is placed in. When a given fiber penetrates any edge of the sphere, a score of 1 is assigned. (**B**) Illustrative example of DAB-developed hNCAM staining at each level of the z-stack, with its respective outline of the measuring sphere. (**C**) Location of the A9 and A10 target structures from which z-stacks were obtained for quantitative analysis of either hNCAM (**Figures 6A, 6B** and **Figure 7H**), or TH^+/$hNCAM^+$ fiber density (**Figures 6D** and **6E**).

Central = central CPu; Cing. C. = cingulate cortex; Dors. lat. = dorsolateral CPu; Dors. med. = dorsomedial CPu; ILC= infralimbic cortex; MFB = medial forebrain bundle; NAc core= core of the nucleus accumbens; Olf. tub. = olfactory tubercle; Sept. = septum.

Figure S6

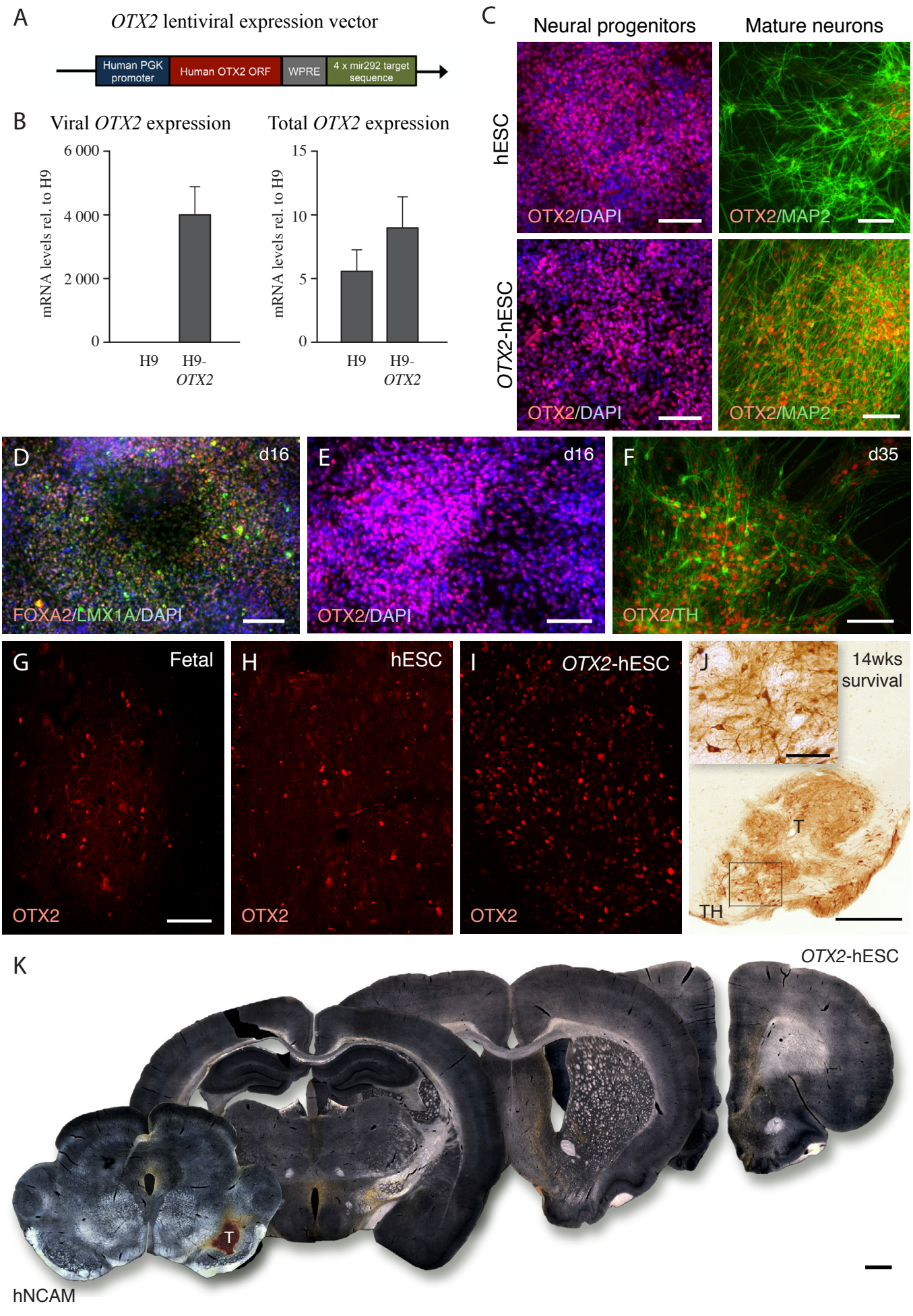
A
OTX2 lentiviral expression vector
Human PGK promoter
Human OTX2 ORF
WPRE
4 x mir292 target sequence
B
Viral OTX2 expression
Total OTX2 expression
mRNA levels rel. to H9
6 000
4 000
2 000
0
15
10
5
H9
H9-OTX2
C
Neural progenitors
Mature neurons
hESC
OTX2-hESC
OTX2/DAPI
OTX2/MAP2
D
d16
FOXA2/LMX1A/DAPI
E
d16
OTX2/DAPI
F
d35
OTX2/TH
G
Fetal
OTX2
H
hESC
OTX2
I
OTX2-hESC
OTX2
J
14wks survival
T
TH
K
OTX2-hESC
T
hNCAM

Figure S6 – Related to Figure 7

Overview of intranigral grafts of *OTX2*-hESCs, 6 months survival.

(**A**) A schematic of the lentiviral construct used for transgenic expression of *OTX2*. To ensure expression of the OTX2 protein only in differentiated cell populations, the vector was regulated by the pluripotency-specific microRNA, mir292, through the presence of 4 target sequences for mir292 in the 3' UTR of the mRNA. WPRE = Woodchuck hepatitis virus post-transcriptional regulatory element. (**B**) Quantitative RT-PCR was performed on differentiated cells (d16) to verify active transcription of the viral construct. It was further confirmed that total levels of *OTX2* mRNA were not significantly increased in transgenic cells compared to control midbrain-patterned hESC progenitors. (**C**) A differentiation experiment comparing hESCs and *OTX2*-hESCs revealed similar numbers of OTX2-expressing progenitors patterned to a midbrain fate. When allowed to terminally differentiate *in vitro* hESCs were seen to down-regulate OTX2 expression in mature neurons (as assessed by $MAP2^+$ cells), while the transgenic expression construct maintained a high level of protein expression at the same stage (d35). *In vitro* characterization of the *OTX2*-hESCs on the day of transplantation (d16) revealed a midbrain phenotype, as determined by FOXA2 and LMX1A co-expression (**D**), as well as an increase in the number of OTX2-expressing progenitors present within the cultures at the time of grafting (**E**) (compare with **Figure S4D**). (**F**) Long-term culture (d35) revealed that OTX2 over-expression is maintained in mature neurons, and that the cells could differentiate into TH^+ neurons. (**G-I**) Intra-nigral grafts of fetal VM (**G**) and hESCs (**H**) contained only a small fraction of OTX2 expressing cells, whereas a high level of OTX2 protein (**I**) expression was maintained in the cells derived from *OTX2*-hESCs.

(**J**) Maintained expression of OTX2 in these transplants did not affect their ability to give rise to TH^+ neurons with mature morphology after 14 weeks post-transplantation. (**K**) Dark-field coronal sections stained for hNCAM used to generate the schematics in **Figure 7A**. **B** Data are represented as mean ± SEM.

Scale bars: **C-I** = 100 μm; **J** = 0.5 mm, inset in **J** = 100 μm; **K** = 1 mm.

SUPPLEMENTAL EXPERIMENTAL PROCEDURES

Culturing and differentiation of hESCs

Human ESCs H9 (WA09, passage 31–45) (Thomson et al., 1998) were maintained on gamma-irradiated mouse embryonic fibroblasts in DMEM/F12, 20% KSR, 0.05 mM 2-mercaptoethanol, 0.5% Pen/Strep and 10 ng/ml FGF-2 (R&DSystems). The cells were passaged once weekly with EDTA (0.5 mM). Differentiation was performed as described in detail in (Kirkeby et al., 2012b). Briefly, cells were differentiated in 10 μM SB431542 (Tocris), 100 ng/ml Noggin (R&D), 200 ng/ml SHH-C24II (R&D) and 0.8 μM CT99021 (Axon Medchem) from day 0-9 of differentiation, using an embryoid body suspension culture for the first 4 days of differentiation. Neural colonies were passaged with accutase on day 11 and kept in medium containing 20 ng/ml brain-derived neurotrophic factor (BDNF), 10 ng/ml glial cell line-derived neurotrophic factor (GDNF), 200 mM ascorbic acid from day 11 until day 16, when the cells were dissociated with accutase and resuspended in HBSS + 0.05% DNAse for transplantation. For *in vitro* terminal differentiation, db-cAMP (0.5 mM) and DAPT (1 μM) was added to the medium from day 14.

Lentiviral expression of OTX2 in hESCs

The open reading frame for human *OTX2* was cloned into a previously described 3rd generation lentiviral construct containing 4 target sites for the microRNA mir292 in the 3' UTR (Sachdeva et al., 2010). High-titer lentiviral particles were produced as described in (http://www.ncbi.nlm.nih.gov/pubmed/9765382), and hESCs were infected at a multiplicity of infection (MOI) of 1:50. The polyclonal OTX2-mirT292

cell line was assessed for transgene expression, and the cells were differentiated as described above.

Immunocytochemistry and qRT-PCR analysis of hESCs

Prior to transplantation, correct VM specification of the differentiated hESCs was verified through immunochemical staining for OTX2, LMX1A and FOXA2 (see antibody specifications below), as well as quantitative RT-PCR using a panel of neural markers as described in (Kirkeby et al., 2012a). For verification of transgenic *OTX2* expression, viral-specific primers were used: Fwd: TCCCATGACCTATACTCAGGCT Rev: CCACATAGCGTAAAAGGAGCA.

Surgical procedures

All rats received a 6-OHDA lesion of the MFB as described in (Kirik et al., 1998).

For intrastriatal transplants of hESCs, a single deposit of 150 000 cells was transplanted to the striatum in a volume of 2 µl, at a concentration of 75 000 cells/µl, to the following co-ordinates relative to bregma: A/P +0.8; M/L +3.0; D/V (from dura) -4.0; tooth bar -3.3. For intrastriatal transplantation of fetal cells a preparation of 2 VMs (6 and 7.5 week p.c.) was dissociated and made to a final volume of 80 µl. 12 µl of which was transplanted to the striatum at the following co-ordinates: A/P +1.2; M/L -2.6; D/V -5.0 (3 µl) and -4.0 (3µl); and A/P +0.5; M/L -3.0; D/V -5.0 (3 µl) and -4.0 (3µl); tooth bar -2.4.

For intranigral transplantation of hESCs, 100 000 cells were transplanted in a volume of 2 µl with a concentration of 50 000 cells/µl on day 16 of differentiation at the following co-ordinates relative to bregma: A/P -4.6; M/L -2.2; D/V -7.0; tooth bar -2.4. Fetal VM, from individual fetuses aged 5.5 or 8 weeks p.c., was dissociated in 20 µl and 1.5 µl per rat was transplanted to the same co-ordinates.

Magnetic resonance imaging

T2-weighted images were acquired for each individual animal using a fast spin-echo sequence with the following parameters: TE, 20 ms; TR, 7000 ms; field of view, 38.4 × 38.4 mm; matrix, 256 × 256; resulting in a 150 × 150 µm in-plane resolution; 38 coronal slices with 300 µm thickness; acquisition time of 12 min.

In vivo LASER spectra were acquired from a single voxel spectroscopy (VOI, 3x3x3=27mm^3) centered within striatal graft. The placement of the MR spectroscopy volume of interest (square box) was determined using coronal T2-weighted images. All 1H-MRS spectra were obtained from the grafted striatum. The prominent peaks of biological importance in our study were those of the neuron-specific compound (NAA+NAAG), the Choline-containing compounds tCho (GPC+PCho) and myo-inositol-containing compounds.

The LCModel fitting software (Stephen Provencher, Inc., Oakville, ON, Canada) was used to quantify the metabolites in the frequency domain, using the basis set as discussed previously (Pfeuffer et al., 1999).

MicroPET imaging

Magnetic resonance imaging (MRI) was performed on a horizontal bore 7T system (Varian-Agilent Technologies) equipped with a gradient coil reaching 600 mT/m (120 μs rise time), a radiofrequency birdcage 1H coil for transmission, and a four-channel surface receive coil (Rapid Biomedical). MRI was used to follow the growth of transplanted cells within 6-OHDA-lesioned striatum to perform MR spectroscopy within graft area and to define anatomical regions of interest (ROIs) through PET/MRI coregistration.

Unilateral 6-OHDA-denervated athymic nude rats were scanned on a Concorde Focus 220 camera (Siemens) dedicated to small-animal imaging with a spatial resolution of 1.35 mm full-width at half maximum. They were imaged before and 5-6 months after hESC transplantation using [18F]-Fallypride and [18F]-LBT999 as radioligands to study post and pre-synaptic DA neurotransmission, respectively. All grafted rats were imaged using the 18 kDa translocator protein (TSPO) specific ligand [18F]-DPA-714 before sacrifice in order to detect any microglial activation associated with graft transplantation.

All imaging experiments were performed on spontaneously breathing rats anesthetized by a gaseous mixture of 100% O2 and isoflurane (induction 4%; maintenance 1.5-2%). Body temperature was continuously monitored using a rectal temperature probe and maintained normothermic (37.5°C) using a feed-back coupled heating blanket (Blanket Control Unit, Harvard Apparatus Limited®, Edenbridge, Kent, UK). The breathing rate of the animals was visually inspected. The rat's head was fixed in flat-skull position using a stereotactic device. Although different

stereotactic devices were used for MRI and PET imaging, the rat's head was fixed in a similar position, allowing the co-registration of the different imaging modalities.

Concomitantly with a bolus injection of [18F]-Fallypride (~1mCi) or [18F]-LBT999 (~1mCi) via a 26-gauge catheter in the tail vein, a 120 min emission scan was performed with an energy window of 350–750 keV and a coincidence time window of 6 ns. The attenuation correction factors of the animal bed were measured using an external Cobalt-57 point source; whereas attenuation correction from the animal was calculated from the emission scans. Finally, the emission sinograms (i.e. each frame) were normalized, corrected for attenuation, scatter and radioactivity decay, and reconstructed using FORE and OSEM 2D (16 subsets and 4 iterations).

PET time frames collected were summed and manually coregistered to the T2-weighted MRI for each animal, using rigid transformations. Coaligned MR images were used to define ROI (left striatum = Intact; right striatum = lesioned+grafted), based on anatomical landmarks, using an in-house image processing software (Anatomist, visualization tool of BrainVISA, http://www.brainvisa.info). This process was performed by the same operator for all experiments. The mean activity concentration values in the left and right ROIs were calculated and used to obtain regional time activity curves (TACs). These curves were then normalized for injected dose and body weight and expressed as percentage standardized uptake values (SUV): %SUV = [100 × ROI values (Bq/ml)]/[(injected dose (mCi) × 37.106)/body weight (g)].

Immunohistochemistry

All rats received a terminal dose of anesthesia 60 mg/kg sodium pentobarbitone i.p. (Apoteksbolaget, Sweden), once animals were fully anesthetized they were trans-cardially perfused with 50 ml saline, followed by 250 ml ice-cold 4% paraformaldehyde. The brains were removed and post-fixed for 2 hours before being transferred to 25% sucrose in PBS. After 48 hours equilibration the brains were sectioned on a freezing microtome (Leica) at a thickness of 35 μm in a 1:8 series.

All immunohistochemistry was performed using free-floating sections that were incubated with primary antibodies overnight at room temperature, or over 48 hours at 4°C, in an incubation solution of 0.1 M phosphate buffered saline with potassium containing 5% normal serum (for the species specific to the secondary antibody) and 0.25% Triton X-100. Secondary antibodies were diluted in the same incubation solution as above for 1 hour at room temperature. Detection of the primary–secondary antibody complexes was achieved by peroxidase driven precipitation of di-amino-benzidine (DAB), or conjugation of a fluorophore (either directly to the secondary antibody or with a streptavidin–biotin amplification step where necessary). All stained sections were mounted on gelatin-coated microscope slides. DAB-developed sections were dehydrated in an ascending series of alcohols before clearing with xylene, and finally coverslipped using DPX mountant. Fluorescent immunostainings were coverslipped using polyvinyl alcohol-1,4-diazabicyclo[2.2.2]-octane (PVA—DABCO), and left to dry overnight.

All secondary antibodies, biotinylated or directly conjugated, were purchased from Vector Laboratories, and used at a concentration of 1:400. Primary antibodies and their respective species and concentrations were used as detailed: rabbit anti-

Calbindin$_{28KD}$ (1:1 000; Swant); rat anti-DAT (1:1 000; Chemicon MAB369); goat anti-FOXA2 (1:500; Santa Cruz M-20); goat anti-GIRK2 (1:200; Millipore ab65096); mouse anti-human NCAM (1:1 000; Santa Cruz Eric-1); rabbit anti-IBA1 (1:1 000; Wako); rabbit anti-LMX1A (1:5 000; Millipore ab10533); goat anti-OTX2 (1:2 000; Neuromics); mouse anti-tyrosine hydroxylase (1:5 000; Immunostar); rabbit anti-tyrosine hydroxylase (1:1 000; Millipore ab152).

Microscopy

All brightfield and darkfield images were captured using a Leica DMI6000B equipped with an automated stage. All fluorescent images we acquired using a TCS SP8 laser-scanning confocal.

Dopamine neuron cell counts

Using DAB-developed immunohistochemistry for TH, all animals in the equipotency experiment were analyzed to estimate the average number of surviving dopaminergic neurons within the graft. For every section of the graft in a given series, the upper and lower focal plane (using a 20x objective on a brightfield microscope) was captured and overlaid to avoid errors in counting the same cell twice. All TH^+ neurons within the graft core were counted and the total number per animal was corrected for the series number.

Dopamine neuron subtype cell counts

A z-stack for the full depth of penetration (>19 μm) was captured for an area covering the entire graft across two sections. From a triple stain, first all TH^+ neurons were quantified separately, then all TH^+ neurons co-expressing either $GIRK2^+$, $Calbindin^+$ or both markers were counted. To account for differences in graft volume between cell sources, quantifications were performed from a section at the beginning of the transplant and at the section occupying the largest area for a given animal. The counts represent the average number of neurons counted from 2 sections of transplants from three randomly selected animals per group.

Fiber density measurements

We adapted the technique described by Mouton and colleagues (Mouton et al., 2002) for quantifying the density of human fibers in a given volume, within a specific A9 or A10 target structure. For quantification of $hNCAM^+$ fiber density in DAB-developed sections, a z-stack was taken at intervals of 1 μm, using a 100x oil-immersion objective on a brightfield microscope (Olympus AX70), generating an image size of 175 μm X 135 μm. For quantification of $hNCAM^+$ and TH^+ fiber density a z-stack with step size of 1 μm was captured on confocal using a 63x water-immersion objective, generating an image size of 138 μm X 138 μm. A given stack was complied using an image analysis software, Velocity v 5.4.2 (Perkin Elmer). Here a sphere with a diameter of 19 μm was created to measure fiber density within the whole z-stack (see schematic in **Figure S5A**). Through the extent of the sphere, the points at which fibers pass through the circumference of the sphere at each z-level (**Figure S5B**). A score of one was given for each fiber crossing. For **Figures 6A, 6B**

and **7H** three, non-over-lapping spheres were analyzed in each stack. In **Figures 6D** and **6E**, one probe was analyzed in all channels (*i.e.* TH, hNCAM, and $TH^+/hNCAM^+$). For each probe the total number of fibers occupying the sphere was expressed as a measure of fiber density within the measured volume.

For fibers passing through the MFB, z-stacks were captured from DAB developed sections stained for hNCAM, that had an area of 23,000 μm^2. This was then corrected to the total area of the MFB for each coronal level at which a z-stack was captured form measurement (-2.92 mm rostral to bregma, Paxinos and Watson, 5^{th} edition).

The A9 and A10 anatomical structures measured are clearly defined in **Figure S5C**, in the coronal levels depicted at (+3.0 mm and +0.72 mm to bregma).

SUPPLEMENTAL REFERENCES

Kirik, D., Rosenblad, C., and Bjorklund, A. (1998). Characterization of behavioral and neurodegenerative changes following partial lesions of the nigrostriatal dopamine system induced by intrastriatal 6-hydroxydopamine in the rat. Experimental neurology *152*, 259-277.

Mouton, P.R., Gokhale, A.M., and Ward, N.L. (2002). Stereological length estimation using spherical probes. Journal of Microscopy.

Pfeuffer, J., Tkac, I., Provencher, S.W., and Gruetter, R. (1999). Toward an in vivo neurochemical profile: quantification of 18 metabolites in short-echo-time (1)H NMR spectra of the rat brain. Journal of magnetic resonance *141*, 104-120.

Thomson, J.A., Itskovitz-Eldor, J., Shapiro, S.S., Waknitz, M.A., Swiergiel, J.J., Marshall, V.S., and Jones, J.M. (1998). Embryonic stem cell lines derived from human blastocysts. Science *282*, 1145-1147.